Chemical Science

Accepted Manuscript

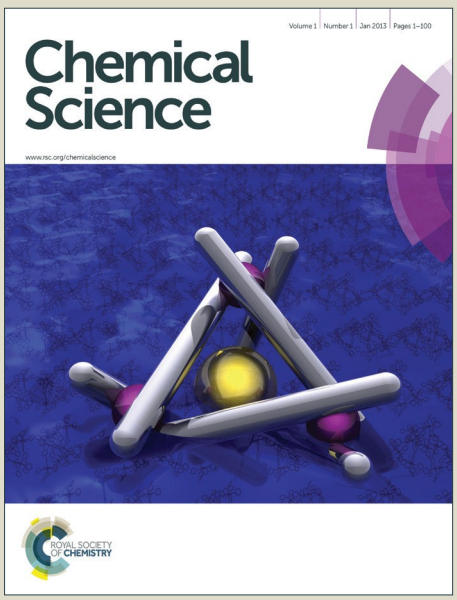

ROYAL SOCIETY OF CHEMISTRY

www.rsc.org/chemicalscience

Cite this: DOI: 10.1039/c0xx00000x

www.rsc.org/xxxxxx

ARTICLE TYPE

Fusing *N*-heteroacene Analogues into One "Kinked" Molecule with Slipped Two-dimensional Ladder-like Packing

Jing Zhang,[‡a] Chengyuan Wang,[‡a] Guankui Long,[a] Naoki Aratani,[b] Hiroko Yamada,[b] Qichun Zhang*[a,c]

Received (in XXX, XXX) Xth XXXXXXXXX 20XX, Accepted Xth XXXXXXXXX 20XX

DOI: 10.1039/b000000x

An unexpected "kinked" N-heteroacene with the slipped two-dimensional ladder-like packing feature is produced from the conventional condensation reaction. The as-obtained compound [2,2']bi(5,12-bis(TIPS)piperazin-3-one[2,3-b]phenazine) (2BPP) consists of two identical backbones (5,12-bis(TIPS)piperazin-3-one[2,3-b]phenazine), which are fused together through a C=C double bond and two intramolecular H-bonds. The study on charge carrier transport indicates that 2BPP single crystal has a hole mobility up to 0.3 $cm^2 V^{-1} s^{-1}$, while theoretical calculation suggests that this compound might possess potential well-balanced ambipolar charge-transport characteristics.

In past decades, polycyclic aromatic hydrocarbons (PAHs) and *N*-heteroacene derivatives have attracted a lot of attentions, with widely investigation in organic field-effect transistors (OFETs), organic resistance memories (ORMs), organic light-emitting diodes (OLEDs) and organic photovoltaics (OPVs).[1] Pentacene and its soluble analogue 6,13-bis(triisopropylsilylethynyl)pentacene (TIPS-pentacene) are one family of the most popular small-molecule organic semiconductors, exhibiting superior hole transporting mobilities (> 1 $cm^2 V^{-1} s^{-1}$) due to their close intermolecular packing, which is supposed to favor charge carrier transport.[2] Thus, tailoring one molecular structure to achieve a larger π-conjugated system or a more condense packing mode is highly desirable. Longer acenes are presumed to own the enhanced intermolecular π-π overlap in the solid state, which could lead to high charge carrier mobilities.[3] However, the instability of large acenes strongly hampers their applications in organic electronics. To address this issue, two-dimensional (2D) acenes with both more sextets and sufficient stability are proposed. 2D acenes and their derivatives have large, planar π surfaces, which can provide the increased intermolecular surface overlapping and effectively increase electron delocalization, potentially resulting in the enhanced charge carrier transporting properties. For example, single-crystal OFETs of a bistetracene derivative reveals the higher hole mobility up to 6.1 $cm^2 V^{-1} s^{-1}$ with remarkable I_{on}/I_{off} ratio of 10^7.[4] In contrast, *N*-heteroacenes have been investigated to show *p*-type, ambipolar or *n*-type OFET behaviours as the number and position of *N* atoms in the backbone varies.[5] OFETs based on a vacuum-deposited *N*-substituted TIPS-pentacene analogue shows electron mobilities in the range of 1.0–3.3 $cm^2 V^{-1} s^{-1}$ under vacuum and 0.3–0.5 $cm^2 V^{-1} s^{-1}$ in ambient air. To date, most of the explored *N*-heteroacenes are linearly-fused systems, which can be prepared through the condensation reaction between *ortho*-diamine based acenes and *ortho*-diketone, *ortho*-dihydroxy, *ortho*-dicyano, or *ortho*-dihalogen substituted acenes (scheme 1).[6] However, in such synthetic conditions, *N*-heteroacenes with unusual shapes are rarely discovered, not to mention the study of their applications. In this report, we present an unexpected "kinked" N-heteroacene with a ladder-like packing feature, which was prepared from the conventional condensation reaction. Its new zigzag structure, physical properties and charge transport capability have been carefully investigated.

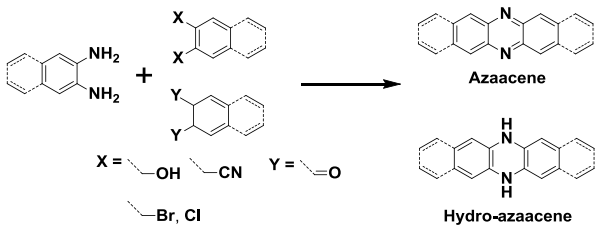

Scheme 1. Representative synthetic route to linearly fused *N*-heteroacenes.

In our previous study, we have already reported that linearly-fused *N*-heteroacene **THNQ** (shown in scheme 2) can be prepared through the condensation reaction between 1,4-bis(TIPS)-2,3-diaminophenazine (**BTDP**) and hexaketocyclohexane (**HKCH**), in which we believe that the steric effect of TIPS group plays a crucial role.[7] Continuing on this direction, we further studied the reaction between smaller 1,4-bis(TIPS)-acene-2,3-diamines and **HKCH**.[8] Surprisingly, when the short 1,4-bis(TIPS)-diaminonaphthalene was used as the starting material, both the star-shape compound (all the carbonyl groups substituted by *N* atoms in yield of 26%) and the linearly-fused product (yield of 17%) were obtained. These results suggest that there might have other factors behind the steric effect, which could also affect the condensation reaction between **BTDP** and **HKCH**. In this situation, we might miss some important unknown *N*-heteroacene products. Thus, we reinvestigated this type of reaction and discovered a meaningful "kinked" compound [2,2']bi(5,12-bis(TIPS)piperazin-3-one[2,3-*b*]phenazine) (**2BPP**). To the best of our knowledge, this is the first report of the generation of a meaningful "kinked" *N*-heteroacene through the conventional substitution reaction.

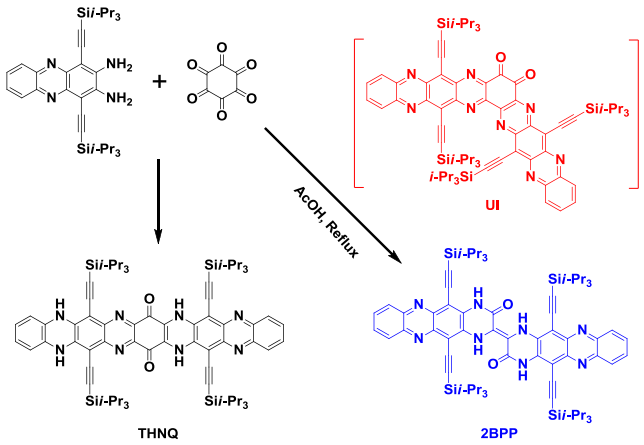

Scheme 2. Synthetic route to **2BPP**.

As shown in scheme 2, the formation of **2BPP** might undergo an unstable intermediate (**UI**) step, in which the diketone could be eliminated instead of participating in the further condensation reaction with amine groups. The as-formed intermediate could be converted into final product **2BPP** through rotation and radical pathway (initiated by light). The possible mechanism has been provided in supporting information (**Scheme S1**). Note that the proposed mechanism is different from previously reported mechanism to eliminate diketone.[9] The novel **2BPP** was obtained in a low yield of 2.3% and was fully characterized by high-resolution mass (HR-MS) spectra, ^{1}H NMR and ^{13}C NMR spectra, and single-crystal analysis. It is noteworthy that two 5,12-bis(TIPS)piperazin-3-one[2,3-*b*]phenazine moieties are linked together by one double bond, which makes **2BPP** fully π-conjugated along the backbone. In addition, the expected H-bonds along both sides were assumed to stabilize the large heteroacene system.

Single crystals (CCDC: 1420681) of **2BPP** suitable for single-crystal X-ray diffraction analysis were obtained by diffusing the poor solvent acetonitrile into toluene solution. **2BPP** crystallizes in a triclinic unit cell, space group P-1(2). The molecular structure of **2BPP** is shown in Figure 1a. The length of the bond between C2 and C2' atoms is 1.35 Å, which is identical to the length of common C=C bond (1.35 Å), suggesting that the two (5,12-bis(TIPS)piperazin-3-one[2,3-*b*]phenazine, **BPP**) moieties are connected by C2=C2' bond. The distance between H1 and O1 or H1' and O1' is 1.95 Å, indicating the existence of intramolecular H-bond. Clearly, the formation of the intramolecular H-bonds with a six-member ring configuration is helpful to stabilize the planar molecular shape and supports the electron delocalization. In fact, the as-prepared molecule possesses a good planarity from side view (Figure 1b). Only a slight twist of **2BPP** can be observed, and the dihedral angel between **BPP** moiety and the C2=C2' bond is ~2.42°. As shown in Figure 1 c, **2BPP** exhibits a slipped 2-D π-stacking motif, similar to that observed for some soluble TIPS-pentacene derivatives. The interplanar distance in **2BPP** is ~3.27 Å along *b* axis, less than that of the typical distance for van der Waals interaction, while the centre-to-centre distance between two adjacent molecules is ~14.65 Å. The slipping angle of two adjacent π-conjugated **BPP**s is ~45°, contributing to significant molecular overlap and ensuring the strong π-π interaction. While view along *a* axis, the distance between two adjacent molecules is ~3.33 Å and in this stack mode, the characterized centre-to-centre distance is about 17.61 Å and much smaller slipping angle (~30°) of two interactional individual **BPP**s leading to poorer electronic coupling is discovered. **2BPP** molecules interact with each other to form two-layer **BPP** units. The face-to-face stacking mode results in the overlapping between the second layer units and the first layer **BPP**s (Figure 1d).

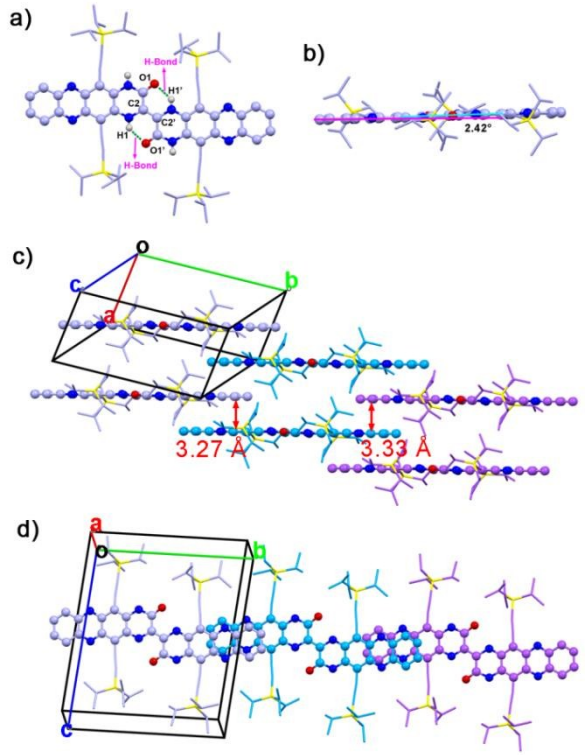

Figure 1. a) Top & b) side view of **2BPP** molecular structure (green dash lines represent the intramolecular H-bond). c) Interlayer distance between neighbouring molecules. d) View of molecular stacking along the *a* axis.

Figure 2a is the UV-vis absorption spectrum of **2BPP** in CH_2Cl_2. **2BPP** has two maximum absorption bands with the maximum absorption at 627 nm and 685 nm. The onset of absorption is 725 nm, which can determine the optical bandgap (E_g) to be 1.71 eV. The strong absorption from 650 nm to 725 nm is similar to that of other hydro-azaacenes, which probably comes from the intramolecular charge transfer. The electrochemical properties of 2BPP were investigated by cyclic voltammetry (CV, Figure 2b). Unlike other hydro-azaacenes, **2BPP** shows no obvious oxidative peaks. One irreversible reductive peak can be observed with onset potential (vs. Fc^{+}/Fc) of -1.29 V, which determines the LUMO level of **2BPP** to be -3.51 eV. The HOMO level was calculated to be -5.22 eV from the LUMO level and E_g. The geometry structure of **2BPP** was optimized by DFT calculations (B3LYP/6-31G*),[10] and the frequency analysis was followed to assure that the optimized structures were the stable states. As shown in Figure S3, the LUMO coefficient delocalizes on the whole conjugated backbone, while HOMO coefficient mainly distributes on the middle electron-rich area. Table 1 summarized the experimental and theoretical calculated energy levels of

2BPP. In both experimental and theoretical calculated results, **2BPP** owns relatively high HOMO levels (-5.22 eV for experimental, and -5.02 eV for calculated result) and a moderate band gap, which indicates **2BPP** could be used as a promising suitable semiconducting material.

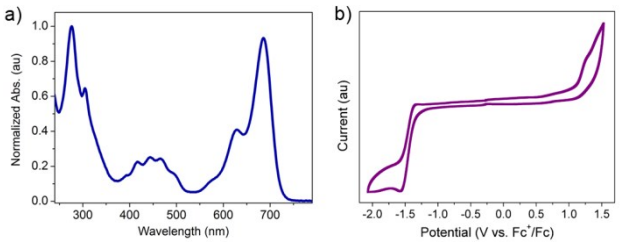

Figure 2. a) Normalized UV-vis absorption spectrum of **2BPP** in CH_2Cl_2. b) Cyclic voltammetric (CV) curves of **2BPP** in anhydrous CH_2Cl_2.

*Table 1. Summarized energy levels of **2BPP**.*

Value	HOMO (eV)	LUMO (eV)	E_g (eV)
Experimental	-5.22	-3.51	1.71
Calculated	-5.02	-2.99	2.04

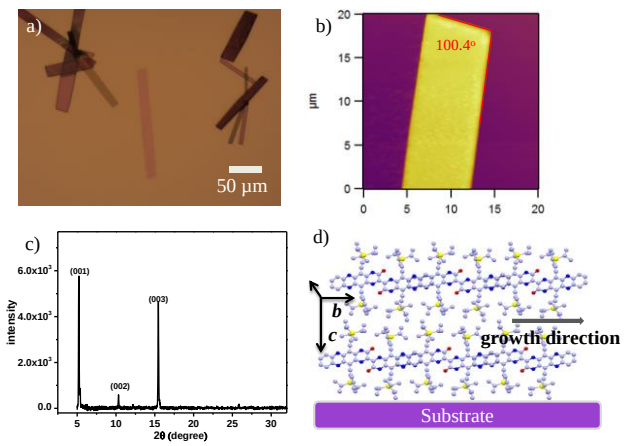

Figure 3. a) Optical and b) AFM images of self-assembled micro/nanoribbons obtained by solution process. c) XRD spectrum of the as-obtained micro/nanoribbons. d) The proposed packing mode of **2BPP** in ribbons on the substrate.

Crystalline ribbons of **2BPP** were grown on octadecyltrichlorosilane (OTS)-treated SiO_2/Si substrate by a drop-casting method. OTS was used to form a siloxane self-assembled monolayer (SAM) on the SiO_2 layer, which could promote and facilitate molecular self-organization during the growth of ribbons. The optical and AFM images in Figure 3a and 3b show that **2BPP** ribbons display a rhombic shape with unambiguous boundaries, indicating the high quality of the ribbons. The as-obtained micro/nanoribbons are several to tens of micrometers in width, and several tens to hundreds micrometers in length. Three sharp and strong diffraction peaks at 2θ = 5.19, 10.32, 15.45 degrees are observed in the out of plane X-ray diffraction patterns (XRD) (Figure 3c), which could be assigned as (001), (002) and (003) plane, respectively, according to the information from the single-crystal structure. All three peaks in the pattern are well indexed along the (001) lattice plane, indicating that the ribbon-like crystals have high crystallinity. The spacing distance of the (001) plane is 17.13 Å, which is in agreement with the lattice parameter of the *c*-axis (17.27 Å), meaning that the molecules stand up along the *c*-axis with an angle of 73° on the substrate. The major driving force for the self-assembly of π-conjugated material is *π–π* interaction from the adjacent molecules, which causes the superior growth direction to either *a*-axis or *b*-axis. The measured angle of the lamellar crystal is 100.4°, which is consistent with the 100.2° dihedral angle between the (100) and (010) planes in the crystal structure. From the crystal morphology, it can be clearly seen that the primary growth direction is along the π-stacking direction (*b*-axis). In this direction, the slipping angle between the adjacent overlapped 2BPP units and the close contact between adjacent π-scaffolds contribute to the significant molecular overlap and ensure the effective charge transport in *π-π* stacking (Figure 3d). In addition, the intermolecular H-bond interactions are also found in the 2BPP molecule structure, which would support charge tunneling quickly from the first half to the second half. The *π-π* stacking direction was parallel to the substrate surface according to the single crystal structure, which make us believe that this high ordered stacking mode with a feasible *π*-electron pathway favors the effective charge transport.

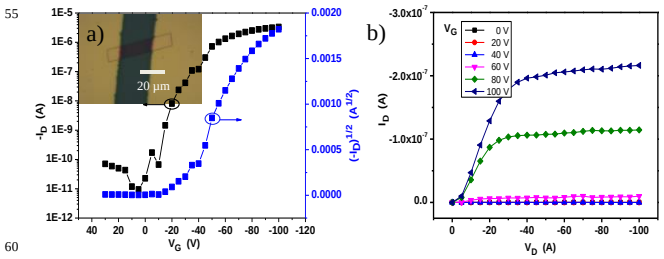

Figure 4. a) Typical transfer curve and b) output curve of single **2BPP** ribbon transistors (insert, optical image of the device with an individual single crystal).

The crystalline ribbons grown on the substrates were fabricated as the top-contact, bottom-gate configuration transistors. The gold source and drain electrodes were deposited with copper masks covering the selected ribbons. With this simple method, 50 nm Au was deposited on the covered substrate; and then, the masks were removed from the ribbon surface and the ribbon devices with the length about 20μm were manufactured. The electrical characteristics of the devices were measured at ambient conditions. The transfer and output curves are displayed in Figure 4a and 4b. The field-effect mobility (μ) was extracted from the saturation regime, and the mobility was calculated by linear fitting of $(I_{DS})^{1/2}$ vs V_G curves. Nearly 50 transistors have been measured and all devices exhibited good gate modulation. According to the transfer characteristics, the mobility was probed at the range of 0.008-0.3 $cm^2\ V^{-1}\ s^{-1}$ along the *b*-axis, the best hole mobility could reach 0.3 $cm^2\ V^{-1}\ s^{-1}$ with the threshold voltage (V_T) of -10~-25 V and on-to-off current ratios (I_{on}/I_{off})> 10^5.

To understand the structure-property relationship of **2BPP**, the Marcus electron transfer theory and an incoherent Brownian

motion model have been employed to calculate the hole and electron mobility (see SI) based on the single-crystal structure of **2BPP**.[11] The room temperature hole and electron-diffusion mobilities were predicted to be 1.49 $cm^2 V^{-1} s^{-1}$ and 1.65$cm^2 V^{-1} s^{-1}$ (Figure S4 and Table S1). The simulated hole mobility is in consistent with the measured mobility of 0.3 $cm^2 V^{-1} s^{-1}$, and π-π stacking directions show the largest transfer integrals for hole transport of 39.92 meV, which is even close to the most famous *p*-type semiconductors (**BTBT**) with transfer integral of ca. 60 meV. Although the material has been predicted to possess well-balanced ambipolar property, electron transport was not apparently observed and the measured mobility was relatively low. However, we believe that with proper modification of this specific heterocyclic molecule or tuning the device fabrication conditions, the ambipolar and good transport character could be realized.

In conclusion, we have presented the synthesis and full characterization of an unexpected "kinked" *N*-heteroacene (**2BPP**), in which two **BPP** units are fused together through a C=C double bond and two H-bonds. Single crystal X-ray study has demonstrated that **2BPP** is a near coplanar molecule with close intermolecular interactions. For the double-layer structure, the face-to-face stacking mode results in the overlap between the second layer **BPP** unit and the first layer unit of the second **BPP** molecule, forming a ladder-like corrugate. The electronic structure calculations suggest the unique large heterocyclic molecule could exhibit good intrinsic ambipolar charge transport property. Experimentally, single-crystal FETs with charge carrier mobilities of 0.3 $cm^2 V^{-1}s^{-1}$ and current on/off ratios of 10^5 have been realized. Further studies on the mechanism of this unusual compound as well as the hydrogen bonding supramolecular synthons would provide more insights to design and prepare novel large conjugated heteroacenes with unique properties.

Acknowledgements

The authors thank Mr. Changli Chen and Prof. Zhigang Shuai from Tsinghua University for their assistance in the transfer integral calculation. The authors thank Prof. Andrew Grimsdale for his value discussion on mechanism. Q.Z. acknowledges the financial support AcRF Tier 1 (RG 133/14) and Tier 2 (ARC 2/13) from MOE, CREATE program (Nanomaterials for Energy and Water Management) from NRF, Singapore. H.Y. acknowledges the financial support by Grants-in-Aid for Scientific Research (KAKENHI) Nos. 25288092, 26620167 and 26105004 from the Japan Society for the Promotion of Science (JSPS).

Notes and references

[a]*School of Materials Science and Engineering, Nanyang Technological University, Singapore, 639798, Singapore. E-mail:* qczhang@ntu.edu.sg

[b]*Graduate School of Materials Science, Nara Institute of Science and Technology, Ikoma, 630-0192, Japan.*

[c]*Division of Chemistry and Biological Chemistry, School of Physical and Mathematical Sciences, Nanyang Technological University, Singapore, 637371, Singapore.*

†Electronic Supplementary Information (ESI) available: [Details of experimental procedure, High-Resolution Mass, ^1H NMR, ^{13}C NMR, Computational Methodology]. See DOI: 10.1039/b000000x/

‡These authors contributed equally to this work.

1. (a) J. E. Anthony, *Chem. Rev*., 2006, **106**, 5028–5048; (b) J. E. Anthony, *Angew. Chem. Int. Ed.*., 2008, **47**, 452–483*;* (c) U. H. F. Bunz, *Acc. Chem. Res.*, 2015, **48**, 1676-1686; (d) U. H. F. Bunz, J. U. Engelhart, B. D. Lindner and M. Schaffroth, *Angew. Chem. Int. Ed.*, 2013, **52**, 3810-3821; (e)) J. B. Li and Q. Zhang, *Synlett*., 2013, **24**, 686; (f) J. Li and Q. Zhang, *ACS Appl. Mater. Interfaces*, 2015, DOI: 10.1021/acsami.5b00113; (g) F. Schlütter, F. Rossel, M. Kivala, V. Enkelmann, J.-P. Gisselbrecht, P. Ruffieux, R. Fasel and K. Müllen, *J. Am. Chem. Soc.*, 2013, **135**, 4550-4557; (h) H. Dong, X. Fu, J. Liu, Z. Wang and W. Hu, *Adv. Mater.*, 2013, ***25***, 6158-6183; (i) Y. Zhao, Y. Guo and Y. Liu, *Adv. Mater*., 2013, **25**, 5372-5391; (j) C. Wang, J. Wang, P.-Z. Li, J. Gao, S. Y. Tan, W.-W. Xiong, B. Hu, P. S. Lee, Y. Zhao and Q. Zhang, *Chem. Asian J*., 2014, **9**, 779-783; (k) C. Wang, B. Hu, J. Wang, J. Gao, G. Li, W.-W. Xiong, B. Zou, M. Suzuki, N. Aratani, H. Yamada, F. Huo, P. S. Lee and Q. Zhang, *Chem. Asian J*., 2015, **10**, 116-119; (l) G. Giri, E. Verploegen, S. Mannsfeld, S. Atahan-Evrenk, D. H. Kim, S. Y. Lee, H. A. Becerril, A. Aspuru-Guzik, M. F. Toney and Z. Bao, *Nature*, 2011, **480**, 504-508; (m) A. L. Briseno, S. C. B. Mannsfeld, M. M. Ling, R. J. Tseng, S. H. Liu, C. Reese, M. Roberts, Y. Yang, F. Wudl and Z. Bao, *Nature*, 2006, **444**, 913-917.

2. (a) M. Watanable, Y. J. Chang, S.-W. Liu, T.-H. Chao, K. Goto, Md. M. I. C.-H. Yuan, Y.-T. Tao, T. Shinmyozu and T. J. Chow, *Nat. Chem.*, 2012, **4**, 574-578; (b) J. Xiao, H. M. Duong, Y. Liu, W. Shi, L. Ji, G. Li, S. Li, X. Liu, J. Ma, F. Wudl and Q. Zhang, *Angew Chem. Int. Ed.*, 2012, **51**, 6094-6098; (c) O. D. Jurchescu, J. Baas and T. T. M. Palstra, *Appl. Phys. Lett.*, 2004, **84**, 3061-3063; (d) J. E. Anthony, J. S. Brooks, D. L. Eaton and S. R. Parkin, *J. Am. Chem. Soc.*, 2001, **123**, 9482-9483; (e) Q. Zhang, Y. Divayana, J. Xiao, Z. Wang, E. R. T. Tiekink, H. M. Doung, H. Zhang, F. Boey, X. Sun and F. Wudl, *Chem. Eur. J.*, 2010, **16**, 7422-7426; (f) J. Xiao, Y. Divayana, Q. Zhang, H. M. Doung, H. Zhang, F. Boey, X. Sun and F. Wudl, *J. Mater. Chem.*, 2010, **20**, 8167-8170.

3. (a) M. M. Payne, S. R. Parkin and J. E. Anthony, *J. Am. Chem. Soc*., 2005, **127**, 8028-8029; (b) D. Chun, Y. Cheng and F. Wudl, *Angew. Chem. Int. Ed.*, 2008, **47**, 8380-5; (c) B. Purushothaman, S. R. Parkin and J. E. Anthony, *Org. Lett.*, 2010, **12**, 2060-2063; (d) C. Tonshoff and H. F. Bettinger, *Angew. Chem. Int. Ed.*, 2010, **49**, 4125-8; (e) B. D. Lindner, J. U. Engelhart, O. Tverskoy, A. L. Appleton, F. Rominger, A. Peters, H.-J. Himmel and U. H. F. Bunz, *Angew. Chem. Int. Ed.*, 2011, **50**, 8588-8591.

4. (a) L. Zhang, Y. Cao, N. S. Colella, Y. Liang, J.-L. Brédas, K. N. Houk and A. L. Briseno, *Acc. Chem. Res.*, 2015, **48**, 500-509; (b) L. Zhang, A. Fonari, Y. Liu, A.-L. M. Hoyt, H. Lee, D. Granger, S. Parkin, T. P. Russell, J. E. Anthony, J.-L. Brédas, V. Coropceanu and A. L. Briseno, *J. Am. Chem. Soc*., 2014, **136**, 9248-9251.

5. (a) Q. Miao, *Adv. Mater*., 2014, ***26*** (31), 5541-5549; (b) Q. Tang, D. Zhang, S. Wang, N. Ke, J. Xu, J. C. Yu and Q. Miao, *Chem. Mater*., 2009, **21**, 1400-1405; (c) Z. Liang, Q. Tang, J. Xu and Q. Miao, *Adv. Mater.*, 2011, **23**, 1535-1539; (d) Z. Liang, Q. Tang, R. Mao, D. Liu, J. Xu and Q. Miao, *Adv. Mater.*, 2011, **23**, 5514-5518; (e) Y.-Y. Liu, C.-L. Song, W.-J. Zeng, K.-G. Zhou, Z.-F. Shi, C.-B. Ma, F. Yang, H.-L. Zhang and X.Gong, *J. Am. Chem. Soc.*, 2010, **132**, 16349-16351; (f) M. L. Tang, A. D. Reichardt, N. Miyaki, R. M. Stoltenberg and Z. Bao, *J. Am. Chem. Soc.*, 2008, **130**, 6064-6065; (g) K. Takimiya, S. Shinamura, I. Osaka and E. Miyazaki, *Adv. Mater.*, 2011, ***23*** (38), 4347-4370.

6. (a) G. Li, Y. Wu, J. Gao, C. Wang, J. Li, H. Zhang, Y. Zhao, Y. Zhao and Q. Zhang, *J. Am. Chem. Soc*., 2012, **134**, 20298-20301; (b) O. Tverskoy, F. Rominger, A. Peters, H.-J. Himmel and U. H. F. Bunz, *Angew. Chem. Int. Ed.*, 2011, **50**, 3557-3560; (c) Z. He, D. Liu, R. Mao, Q. Tang and Q. Miao, *Org. Lett*., 2012, **14**, 1050-1053; (d) C. Tong, W. Zhao, J. Luo, H. Mao, W. Chen, H. S. O. Chan and C. Chi, *Org. Lett.*, 2012, **14**, 494-497; (e) Z. He, R. Mao, D. Liu and Q. Miao, *Org. Lett.*, 2012, **14**, 4190-4193; (f) P. Gu, F. Zhou, J. Gao, G. Li, C. wang, Q. F. Xu, Q. Zhang and J. Lu, *J. Am. Chem. Soc*., 2013, **135**, 14086–14089.

7. C. Wang, J. Zhang, G. Long, N. Aratani, H. Yamada, Y. Zhao and Q. Zhang, *Angew. Chem. Int. Ed.*, 2015, **54**, 6292-6296.

8. (a) J. Li, J. Miao, G. Long, J. Zhang, Y. Li, R. Ganguly, Y. Zhao, Y. Liu, B. Liu and Q. Zhang, *J. Mater. Chem. C*, 2015**, 3,** 19410– 19416; (b) J. Li, S. Chen, P. Zhang, Z. Wang, G. Long, R. Ganguly, Y. Li, and Q. Zhang, *Chem Asian J*. 2015, DOI: 10.1002/asia.201500932.

9. (a) J. Strating, B. Zwanenburg, A. Wagenaar and A. C. Udding, *Tetrahedron Lett.*, 1969, **10**, 125-128; (b) M. B. Rubin and M. Kapon, *J. Photoch. Photobio. A*, 1999, **124**, 41-46; (c) H. Yamada, Y. Yamashita, M. Kikuchi, H. Watanabe, T. Okujima, H. Uno, T. Ogawa, K. Ohara and N. Ono, *Chem. Eur. J.*, 2005, **11**, 6212-6220; (d) H. Yamada, Y. Yamaguchi, R. Katoh, T. Motoyama, T. Aotake, D. Kuzuhara, M. Suzuki, T. Okujima, H. Uno, N. Aratani and K.-I. Nakayama, *Chem. Commun.*, 2013, **49**, 11638-11640.

10 (a) A. Becke, *J. Chem. Phys.*, 1993, **98**, 5648-5652; (b) C. Lee, W. Yang and R. G. Parr, *Phys. Rev. B*, 1988, **37**, 785-789.

11. (a) W. Deng and W. A. Goddard, *J. Phys. Chem. B*, 2004, **108**, 8614-8621; (b) J. L. Bredas, D. Beljonne and V. Coropceanu Cornil, *Chem. Rev.*, 2004, **104**, 4971-5004; (c) R. A. Marcus, *Rev. Modern Phys*., 1993, **65**, 599-610.